Reusing Life-Expired Railway Ballast: Laboratory Testing, Shape Analysis, and Petrographic Evaluation

T. Abadi, Ph.D.[1]; B. N. Madhusudhan, Ph.D.[2]; H. Li, Ph.D.[3]; and L. Le Pen, Ph.D.[4]

Abstract: During its service life, railway ballast degrades. Individual grains are abraded, asperities may break off, and the assembly loses performance as the finer material created progressively fouls the assembly. The causes of this are the repeated cyclic loading from passing trains and the major damage caused to ballast by tamping operations to restore track geometry. Eventually the ballast bed requires complete replacement, and recovered trackbed material is disposed of as waste or downcycled. However, modern ballasts often are formed from stronger parent rocks than in the past, and a proportion may retain sufficient characteristics for reuse. This paper investigated the reuse of recovered life-expired ballast. A series of tests using fresh and reused ballast was carried out using the Southampton Railway Testing Facility (SRTF) and a large triaxial testing apparatus to compare performance. The properties of individual ballast grains were characterized in terms of their shape and petrographic make up. The results show that the type of recovered life-expired ballast used in this study has good performance and similar strength to fresh ballast despite having reduced surface roughness. The petrographic analysis showed that a majority of the recovered ballast was formed of granite, with a significant minority of basalt. These findings may be in contrast to those of some previous studies in which different life-expired rock sources were used, and highlights the importance of the source material. **DOI: 10.1061/(ASCE)GT.1943-5606.0002904.**

Author keywords: Ballast; Shape; Roughness; Triaxial; Railway; Trackbed; Settlement.

Introduction

Ballasted railway track is the primary form of existing railway track system throughout the world and is likely to remain so for the foreseeable future. The general track form consists of Vignoles rails running over concrete or timber sleepers on a trackbed. The trackbed is formed of a typically 300-mm thickness of ballast and sometimes a ~100-mm -thick sand blanket placed upon a prepared subgrade. The thickness of the trackbed is specified to reduce stresses to levels acceptable for long-term cyclic loading of the subgrade (Li and Selig 1998a, b). If the subgrade is of sufficient stiffness and strength, the ballast thickness is at least the depth necessary to carry out tamping operations.

Over its life cycle, ballast is subjected to loads from passing trains. Measured in cumulative tonnage, busy routes commonly can receive more than 15 million equivalent gross t/year (e.g., some sections of the United Kingdom's (UK's) east coast mainline achieve this) (Le Pen et al. 2018). Usage inevitably leads to track geometry deterioration and periodic maintenance to restore line and level for safe and comfortable train running. Maintenance usually is carried out by mechanized tamping, a process in which vibrating tines are introduced vertically on either side of the railseats of the sleepers to squeeze the ballast together, raising the support beneath the railseats, while the rails and sleepers are lifted and held to a design line and level. Although maintenance by tamping may be a necessary activity, it is intensely damaging to the ballast (Selig and Waters 1994; Aingaran et al. 2018). Tamping consists of two motions: a slower, large-amplitude squeezing motion to raise the ballast level; and a second faster, small-amplitude higher frequency vibration of the tines at ~35–40 Hz to allow the times to break the frictional contact between grains and push through the ballast (Aingaran et al. 2018). The squeezing motion rotates the principal stresses from vertical to horizontal, loosening the ballast and causing a reduction in support stiffness and rapid rates of settlement as the newly tamped track beds in. Together, both motions cause abrasion, attrition, and breakage generating fouling material (fines). There may also be environmental sources of fouling such as migration of finer materials from the subgrade. Qian et al. (2022) showed that ballast fouling and the moisture content of the fines affects the strength of the ballast matrix. The damage caused by tamping, the generation of fines, and the addition of environmental fouling leads to an increasing deterioration rate for trackbed performance and requirements for more-frequent maintenance. This partly can be alleviated by ballast cleaning, using specialized machines at midlife cycle, and includes reintroduction of a proportion of fresh ballast to approximately restore the intended particle-size distribution. Ballast cleaning extends the period before ballast replacement. However, eventually, perhaps after a 20–30-year service life encompassing 10–15 tamps and a midlife ballast clean, the trackbed performance becomes so poor that it requires complete replacement, i.e., renewal. During renewal, the now life-expired and fouled ballast is dug out and replaced with fresh ballast.

Railway ballast as a trackbed-forming material has been in use for centuries. It is relatively inexpensive compared with alternative slab tracks (in terms of up-front cost) and offers the potential for the track geometry to be realigned relatively easily. One potential advantage also has been that ballast may be sourced from the nearest local quarry. This latter advantage no longer necessarily holds, because modern railway ballasts preferably are sourced from

[1]Infrastructure Research Group, Univ. of Southampton, Southampton SO16 7QF, UK.

[2]Infrastructure Research Group, Univ. of Southampton, Southampton SO16 7QF, UK (corresponding author). ORCID: https://orcid.org/0000-0002-2570-5934. Email: mbnm1f13@soton.ac.uk

[3]Dept. of Civil Engineering, Univ. of Nottingham, University Park, Nottingham NG7 2RD, UK.

[4]Infrastructure Research Group, Univ. of Southampton, Southampton SO16 7QF, UK.

Note. This manuscript was submitted on November 4, 2021; approved on June 17, 2022; published online on November 12, 2022. Discussion period open until April 12, 2023; separate discussions must be submitted for individual papers. This paper is part of the ***Journal of Geotechnical and Geoenvironmental Engineering***, © ASCE, ISSN 1090-0241.

crushed igneous or metamorphic rocks because of their greater strength and fracture resistance (Watters et al. 1987; Clifton et al. 1987; Raymond 1985). This means that ballast material may be shipped from the most suitable quarries. In the UK this can mean that ballast sourced in Norway or Scotland ends up in the South of England, as was the case for the construction of High Speed 1 (linking London with Paris), for which only ballast sourced from one quarry in the UK (Glensanda) or ballast from Norway was considered to be of sufficient quality. Generally, the types of ballast materials that are used for railway ballast in many parts of the world are required to meet minimum criteria commonly determined from the Los Angeles abrasion (LAA) (BSI 2020) and Micro-Deval (MD) (BSI 2011) tests. Their application to railway ballast is specified in BS EN 13450 (BSI 2002). These are the UK and European standards; other regions apply similar standards with some variations.

The Micro-Deval and the LAA test are different types of abrasion tests. The Los Angeles abrasion test measures ballast particle toughness or tendency for breakage. The Micro-Deval test measures the durability required to achieve the desired ballast life (Selig and Boucher 1990). The specification of both types of tests is perhaps indicative that they provide complimentary but unequal results, so a material may perform better in one test than the other when ranked against other tested materials (Selig and Boucher 1990).

The criteria specified for candidate ballast materials to pass these tests are likely to eliminate sedimentary rocks from consideration leaving common igneous materials such as granites, granodiorites, basalts, and gabbros (the last two commonly are referred to as types of trap rock) as likely suitable ballast materials.

The relatively new understanding of the most-suitable ballast types (on the scale of the history of the railways) has meant that since the 1980s in the UK, sedimentary ballasts previously present on some railway routes gradually have been replaced during renewals with igneous ballasts. With a rollout covering the previous 40 years, there is a strong likelihood that recovered material from renewals taking place today will be an igneous ballast.

In the long-term, quarrying ever greater quantities of raw ballast materials to replace life-expired material is potentially unsustainable (or, at best, simply inefficient), and there is growing pressure on the railway industry to move toward more environmentally acceptable practice. One means to reduce the demand for raw materials is to reuse life-expired ballast.

In the UK, recovered trackbed material from renewals is sent to processing centers where the material is screened, cleaned, and sieved. Depending on its initial quality and degree of fouling material, much of this processed material is of too fine a gradation for reuse as railway ballast but still may be downcycled, for example, as a fill material for the highways industry. However, a portion of the recovered trackbed material is in a suitable size fraction to be reused as ballast.

Reusing ballast offers a potentially more sustainable future for ballast supplies. However, there is concern about the quality of recovered ballast. There are doubts and/or contradictory opinions about its performance. Many practitioners hold that recycled ballast performs less well than fresh ballast. Research and trials in Australia have shown potential benefits for the use of recycled ballast placed when used alongside geocomposites (Indraratna and Salim 2003). They also found ballast breakage and deterioration of strength to be one of the mechanisms explaining degradation in latite (igneous rock) fresh ballast.

This paper investigated the potential for reusing recovered UK life-expired predominantly igneous railway ballast with a small proportion of basalt by means of comparative tests with a fresh igneous railway ballast. Tests used the Southampton Railway Testing Facility (SRTF), a large triaxial testing apparatus at Nottingham University, surface roughness measurements using optical three-dimensional (3D) surface characterization, and material composition tests by the UK's National Oceanography Centre (NOC).

The testing methods can be classified depending on whether they investigate the performance of representative volumes of assemblies of grains—referred to as element tests—or are tests at the grain-scale. The test methods were applied to both used and fresh ballast, and the results were compared.

Materials: Reused and Fresh Ballast

Both fresh and reused ballast were supplied by Network Rail (NR) from stocks held at Eastleigh recycling center, Hampshire, UK. The physical appearance of the two ballast types is shown in Fig. 1. Visually, the fresh ballast was assessed as being entirely from a crushed granite or granodiorite parent rock (Clayton et al. 1995). The used material also was mainly from granite or granodiorite parent rock; however, other rock types also were present, including a proportion of basalt. To quantify the composition of the used ballast, 34 kg of material comprising some 427 individual grains was evaluated visually and the proportions of different rock types were quantified. The reused ballast was found to contain just over 60% granite or granodiorite, 20% basalt, and small proportions of limestone, flint, and miscellaneous particles such as dolomite and volcanic glass (Table 1).

The primary proportion of used ballast material, the granite or granodiorite, is thought to have spent some 20–30 years in the trackbed. The limestone present perhaps was remaining material from a previous trackbed that largely was removed during a previous renewal. The flint and other material present likely were contaminants present in the local soil. The basalt and some portion of the granite material may be additional materials placed during tamping works over the course of the trackbed's life cycle or from a previous life cycle. The provenance of the used ballast and the fresh material

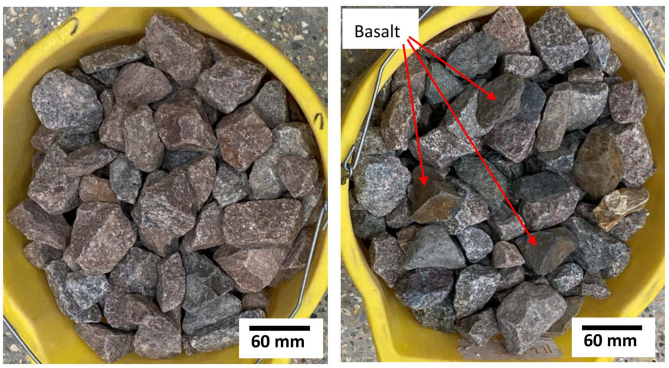

Fig. 1. Physical appearance of (a) fresh ballast; and (b) reused ballast.

Table 1. Proportions of material visually assessed to be present in reused ballast

Visual assessment of grain material	Percentage of total (427 grains) (%)
Granite/granodiorite	63
Basalt	21
Limestone	9
Flint	3
Other	3

Table 2. Ballast commonly available in UK compared with ballast supplied for testing

Ballast source	Parent rock	Specific gravity	LAA (%)	Micro-Deval (%)
Cliffe Hill (Leicestershire, UK)	Granodiorite	2.78	16[a]	6.5[a]
Mount Sorrel (Leicestershire, UK)	Pink granite	2.67	20[a]	7[a]
Eastleigh fresh	Granite/granodiorite	2.67	N/A	N/A
Eastleigh reused	Granite/granodiorite	2.73	N/A	N/A

[a]Values taken from quarry websites.

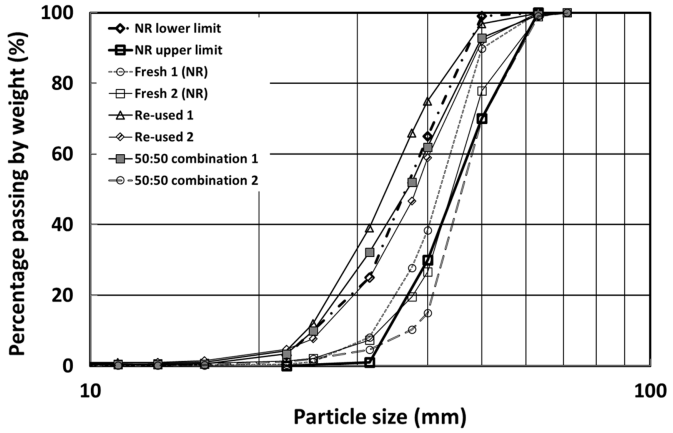

Fig. 2. PSD of the current standard specification of ballast used by Network Rail, fresh and recycled ballasts, and blends of recycled and fresh ballasts tested.

from Eastleigh recycling center was not available. However, the supplied material can be compared with known sources.

Table 2 presents some properties of ballasts commonly available from quarries in the UK. The rock type and its specific gravity were close to those of ballast from a number of UK quarries supplying granite or granodiorite crushed rock ballasts. Sieve tests were carried out to determine the particle-size distributions for comparison with each other and with the current Network Rail ballast specification used in the UK (Fig. 2). Reused ballast 1 was slightly finer than the range normally specified, and Fresh ballast 2 was slightly coarser (Fig. 2). It is not uncommon when receiving relatively small volumes of material that a particular sieved sample is slightly out of the expected range. This can be a result of segregation during transport and also of from the location within a stockpile from which a particular shipment has been collected (finer particles tend to fall to the bottom).

Grain Scale Tests

Grain scale tests and shape measurements were carried out to compare particle mineralogy, form, angularity, and surface roughness.

Ballast Particle Mineralogy

X-ray diffraction (XRD) and thin section analysis techniques are used by geological sciences to determine the mineralogical composition and origin of rock. For X-ray diffraction, fresh and used ballast of different sizes were selected, and a small sample from each grain was taken and pulverized to a powder for analysis (four particles of each mineralogy). Selected ballast particles also were cut into thin sections and analyzed using scanning electron microscopy with energy dispersive X-ray spectroscopy (SEM-EDS) imaging and elemental mapping. Fig. 3 shows the SEM images of the thin section and elemental mapping analysis of both fresh and used ballast. Table 3 presents the average percentage of minerals in fresh and used ballast from both X-ray diffraction and elemental mapping analysis of thin sections. The thin section analysis confirmed that the small powdered XRD samples gave representative results for mineral proportions.

The fresh ballast was mainly granite rather than granodiorite, and the dominant minerals, from analysis of various particles, were quartz and feldspar, followed by mica (biotite) and amphibole, chlorite, and other trace minerals (Table 3). The life-expired granite ballast contained a slightly lower percentage of quartz than did the fresh ballast. The 21% proportion of basalt in the used ballast was formed mainly from quartz.

Watters et al. (1987), provided a table of minerals and their suitability for ballast rock. In their petrographic evaluation, quartz and plagioclase feldspar were of high and moderate suitability, respectively, and also scored highly for hardness, whereas calcite was of lower suitability and lower hardness. The portion of basalt and limestone could influence the overall response of life-expired ballast because the characteristic strength is different from that of the predominant granite particles (Hoek and Brown 1997; Piasta et al. 2017). The used ballast grains perhaps already have had their weaker asperities fractured off, and the remaining intact grains may be expected to have a greater resistance to fracture than the general population of grains initially placed; however, they also likely would have undergone surface smoothing.

Ballast Shape and Surface Characteristics

The shape of the individual grains of a granular material affects their packing, strength, stiffness, and stability or durability (Cho et al. 2006; Potticary et al. 2015, 2016; Madhusudhan and Todisco 2018). Ahmed and Martinez (2021) showed that angular sands have slightly higher strength and a greater rate of dilation than rounded sands. Madhusudhan and Todisco (2018) demonstrated that the surface roughness of particles influences the stiffness of the granular materials. Widely recognized particle-shape descriptors (Fig. 4) are of three types: particle form, roundness (angularity) and surface roughness (Barrett 1980). Particle form is the largest-scale property and may be quantified using a grain's longest (L), intermediate (I), and shortest (S) orthogonal dimensions and combining them in ratios I/L and S/I.

Alternate indexes are available for form. In this paper, form was characterized using a 3D imaging technique using a laser scanner to create a representative point cloud at 50-μm resolution. Arithmetic ellipsoids were fitted onto the point cloud based on locating the volumetric centroid and distances to the surface of the grain (Fig. 5). The longest, intermediate, and shortest lengths of the particle then were obtained from the equivalent ellipsoid fitted in 3D. The ellipsoid fitting method has been applied following methods described by Potticary (2018), Potticary et al. (2014, 2015, 2016),

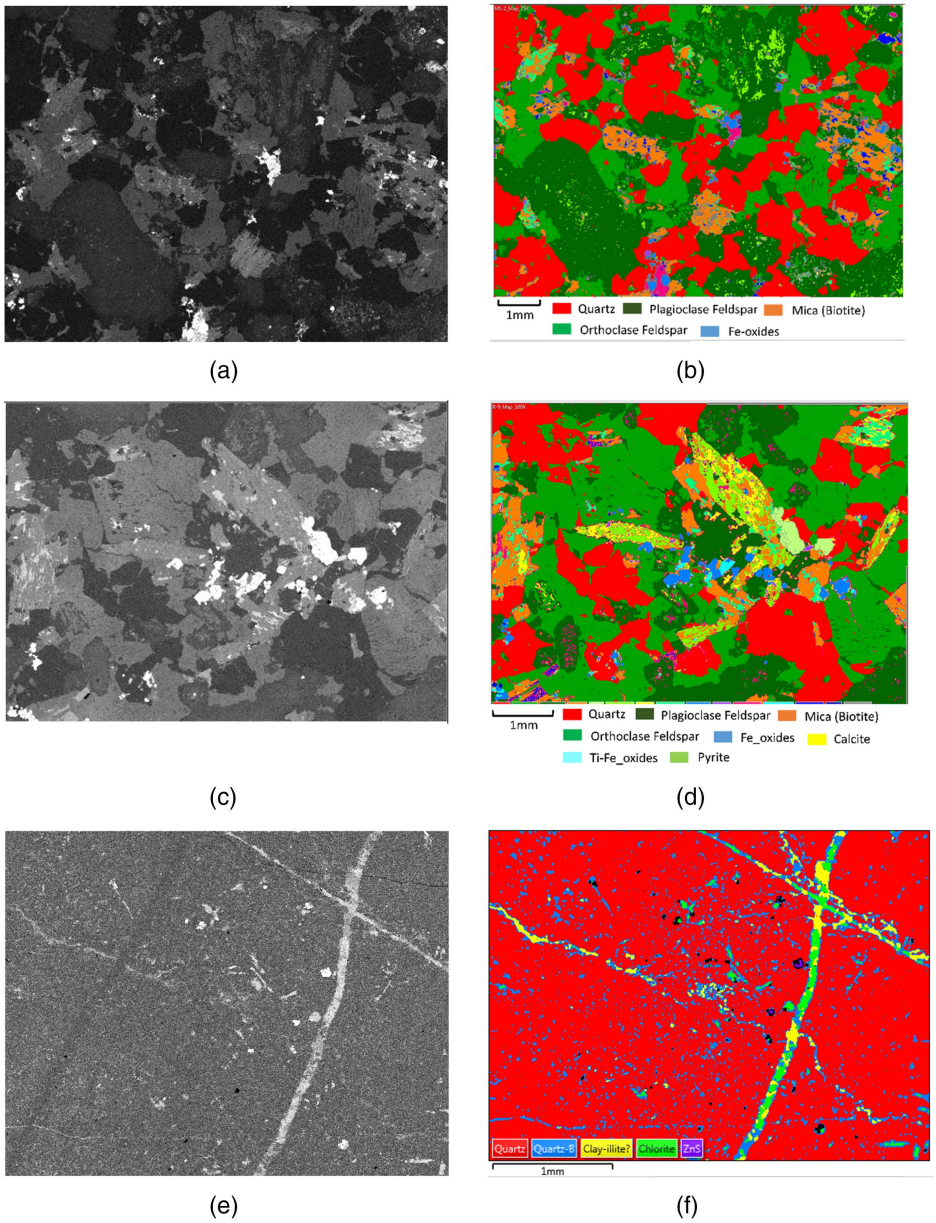

Fig. 3. (a) Fresh ballast SEM image; (b) fresh ballast elemental map; (c) used granite ballast SEM image; (d) used granite ballast elemental map; (e) used basalt ballast SEM image; and (f) used basalt ballast elemental map.

Table 3. Proportions of minerals present from XRD and thin section analyses

	Mineral in X-ray diffraction (four samples each) (%)				Mineral in elemental mapping of sections (four sections each) (%)			
Mineral	Fresh granite	Used granite	Used basalt	Used limestone	Fresh granite	Used granite	Used basalt	Used limestone
Quartz	32.1	26.0	84.5	0.8	31.8	23.1	90.6	0.3
Plagioclase feldspar	38.0	42.2	—	—	33.4	33.6	—	—
Orthoclase (potassium) feldspar	12.3	16.6	4.2	—	19.8	20.6	3.2	—
Mica (biotite) and amphibole	8.0	7.0	8.4	—	7.8	7.4	5.4	—
Chlorite	6.1	1.7	—	—	5.0	7.6	—	—
Calcite	0.4	1.5	—	97.7	—	2.3	—	98.4
Fe oxides	2.0	2.4	1.8	—	1.0	1.9	0.4	—
TiFe oxides	—	1.8	—	—	—	1.9	—	—
Other	1.1	0.8	1.1	1.5	1.2	1.6	0.4	1.3

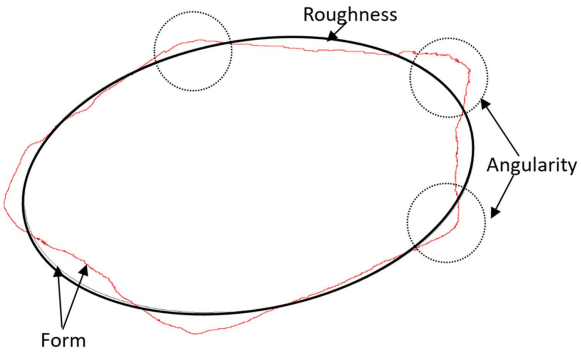

Fig. 4. Ellipse fitting for particle-shape analysis and descriptors in two dimensions.

and Harkness and Zervos (2019). The angularity of the ballast was obtained as the difference between actual particle volume and its equivalent scalene ellipsoid, normalized over actual volume

$$\text{Angularity} = \frac{\text{Volume}_{\text{actual}} - \text{Volume}_{\text{ellipsoid}}}{\text{Volume}_{\text{ellipsoid}}} \quad (1)$$

The ballast particle shape (form) is presented using a Zingg plot (Zingg 1935), expressed as elongation (S/I) versus flatness (I/L) for both fresh and reused ballast (Fig. 6). The solid data points represent the form of fresh ballast of different sizes, whereas the shaded data points represent the reused grains. In general, the fresh ballast was more platy and flat and columnar than the reused ballast, which was more spherical and columnar. Table 4 shows average ratios grouped by grain size. There were small differences in form with grain size, in common with prior findings (Le Pen et al. 2013), but no strong trends. The angularity of fresh ballast consistently was greater in all grain-size ranges compared with used ballast.

Smaller-scale surface roughness influences frictional contact between grains, and thus the strength and stiffness of the assembly (Harkness et al. 2016; Madhusudhan and Todisco 2018). Used granite and fresh granite ballast of different sizes were measured for surface roughness using a varying-focus microscopy technique. Fig. 7 shows close images indicating the roughness of fresh and reused ballast grains. There is a significantly smoother surface on the reused material. The resulting surface profile was analyzed using the power spectral density function, which represents the amplitude of a surface's roughness in terms of spatial frequency within the analyzed area (Gong et al. 2016). The power spectral density function transforms the particle surface roughness of different heights into frequency domain described by wave vector

$$\text{PSD}(q_x, q_y) = \frac{1}{(2\pi)^2} \int \int_{-\infty}^{\infty} C(x,y) e^{-i(xq_x + yq_y)} dxdy \quad (2)$$

where PSD (x, y) = power spectral density function of particle surface; $C(x, y)$ = cross-correlation of surface heights; and q_x and q_y = wave vectors in x- and y-dimensions of surface, respectively (μm^{-1}). The RMS roughness then can be obtained by

$$S_q = \left(2\pi \int_{q_0}^{q_1} \text{PSD}(q) dq\right)^{0.5} \quad (3)$$

The RMS surface roughness of fresh ballast, averaged over 10 different particles was found to vary between 40 and 53 μm, and that for reused ballast varied between 12 and 23 μm. Hence the surface roughness of fresh ballast was found to be as much as 4 times that of reused ballast for grains of similar mineralogy (visually granite). This is logical, because reused ballast has been in a trackbed for perhaps 30 years and has been subjected to significant volumes of traffic loading and multiple tamps. The significance of the greater surface roughness of the fresh ballast perhaps is less than the relative values indicate. Prior work has shown that fresh material abrades and polishes readily, and much of the roughness may come away after a relatively few cycles of loaded contact and this may even explain a softer initial performance (Harkness et al. 2016).

Southampton Railway Testing Facility

Testing Arrangement

To evaluate the comparative performance of the fresh and reused ballast, a series of tests was carried out using the Southampton Railway Testing Facility, a laboratory representation of a single sleeper bay of track (Fig. 8).

The apparatus comprises two vertical sides, constructed from heavy steel sections and panels. These are located on a strong floor and held apart at a fixed distance of 0.65 m in an approximately plain strain condition. In the tests, a ballast bed 300 mm deep is prepared on a 12-mm-thick rubber mat to represent a subgrade. The ballast is compacted, and the geometry of the final configuration is shown in Fig. 8(c). A G44-type sleeper was used in the

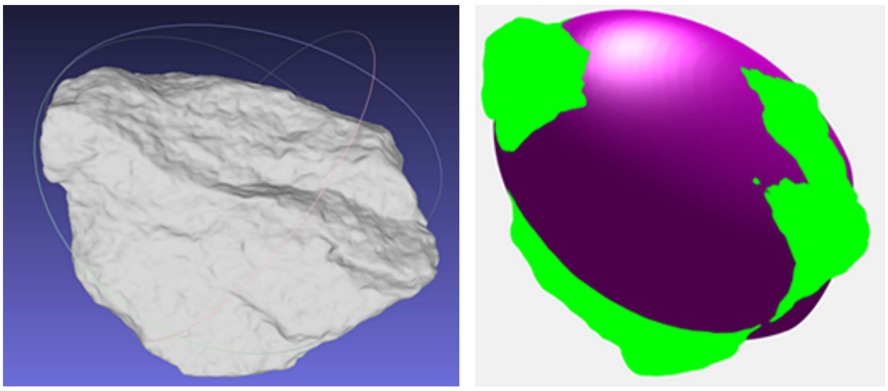

Fig. 5. Three-dimensional shape characterization of ballast particle: (a) ballast particle 3D surface scan; and (b) equivalent arithmetic ellipsoid fitting on the scanned ballast particle.

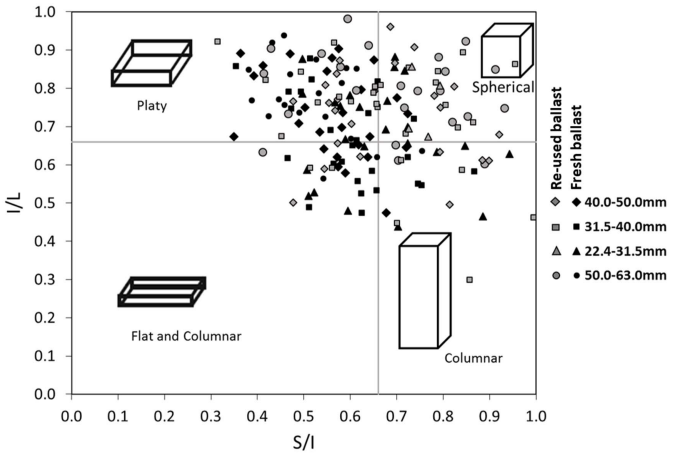

Fig. 6. Zingg plot for fresh and reused ballast. Black data points represent fresh ballast, and grey data points represent used ballast of different sizes.

tests; this is a common type of monoblock steel-reinforced concrete sleeper used in the UK and similar to many used throughout the world. The G44 has major dimensions of 2.5 × 0.285 × 0.2 m (length × width × height), giving a soffit area of 0.713 m^2. Short lengths of rail are fixed to the sleeper using standard fastenings. Load is applied by means of a loading beam spanning the rail tops and in contact with a hydraulic actuator at its midspan [Fig. 7(b)]. The test has been established as a means to compare the relative performance of different sleeper and ballast arrangements. Further details of common test preparation methods were described by Le Pen and Powrie (2011) and Abadi et al. (2015, 2018).

A sinusoidal load of 10 t was applied to represent a 20-t axle load assuming a 50% load transfer. Vertical load distribution from train wheels is transferred through the rails and distributed to each component trackbed beneath the rails. We used beam on elastic foundation (BOEF) analysis to calculate the vertical distribution to the sleepers. The load transferred to the sleeper depends on the sleeper space, rail profile, and ballast stiffness. We calculated this by varying these factors from lower to higher acceptable values, which led to about 50% of wheel load transferred to the sleeper (Abadi et al. 2015). The loading rate was set to 3 Hz to enable the tests to be carried out within a reasonable timescale, achieving 3 million cycles in 12 days. The loading rate maintained a pseudostatic loading regime because peak cyclic accelerations remained well below 1***g***. The choice of 20 t as the target axle load was somewhat arbitrary; most passenger trains have lower axle loads than this, whereas freight loads can be much higher, especially on dedicated freight routes. Nevertheless, by applying a common load for the series of tests, it was possible to gain insights into relative performance.

Instrumentation

To measure ballast permanent and resilient movement throughout the test, 12 vertical LVDTs were placed at locations along the sleeper top (Fig. 9). To determine the average deflection, each LVDT reading was weighted in proportion to the nearest area of sleeper surface, as shown by the shaded regions in Fig. 8.

SRTF Test Plan and PSDs for Tested Materials

The proportions of fresh and reused ballast were varied as either fully fresh, fully reused, or a half-and-half blend. Two tests each were carried out using 100% fresh and 100% reused ballast materials. Subsequently, two tests were carried out using blends of fresh and reused ballast in 50% proportions. Each blended ballast was created by mixing 100-kg batches to ensure uniformity of mixing. Each test required approximately 2 t of material. Further ballast sample material properties for each test are presented in Table 5. The six tests were carried out to at least 4.1 million load cycles, with some tests continued to 4.7 million load cycles (Table 6).

Table 4. Average form of fresh and used ballast

Size range (mm)	No. of grains	Ratio I/L			Ratio S/I			Angularity		
		Used	Fresh	Change (%)	Used	Fresh	Change (%)	Used	Fresh	Change (%)
50–63	22	0.750	0.767	2.3	0.665	0.524	21.2	0.322	0.395	18.4
40–50	25	0.730	0.732	0.3	0.673	0.563	16.3	0.324	0.395	17.9
31.5–40	25	0.728	0.665	8.7	0.680	0.600	11.8	0.337	0.394	14.4
22.4–31.5	25	0.758	0.681	10.2	0.754	0.651	13.7	0.354	0.406	12.8

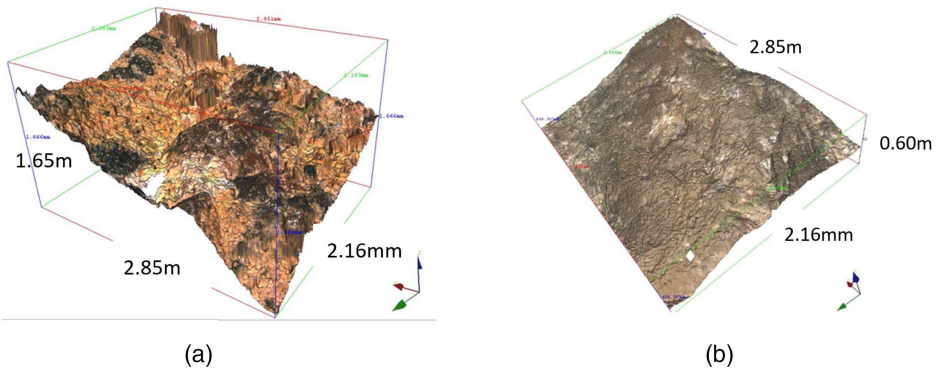

Fig. 7. Surface characterization of ballast particles using varying focus microscopy: (a) fresh ballast surface; and (b) recycled ballast surface.

J. Geotech. Geoenviron. Eng., 2023, 149(1): 04022123

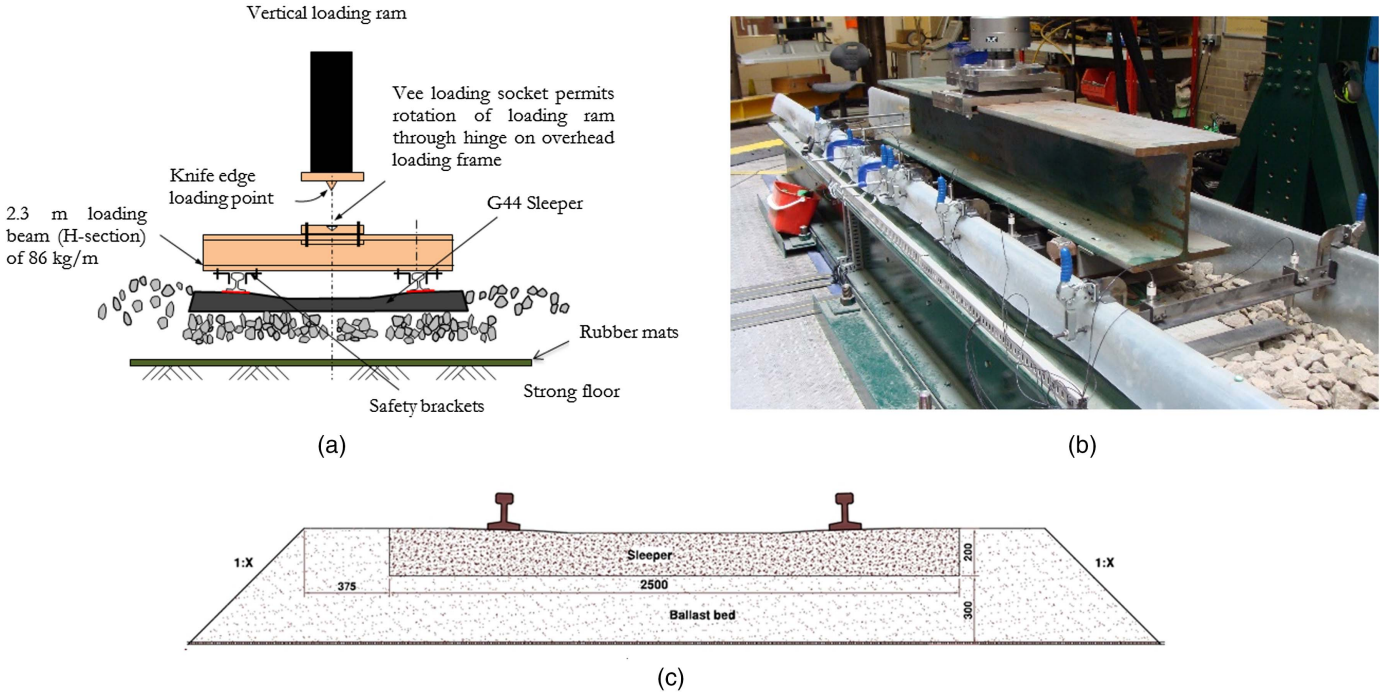

Fig. 8. SRTF laboratory tests: (a) schematic view; (b) photograph; and (c) cross section. (Data from Abadi et al. 2019.)

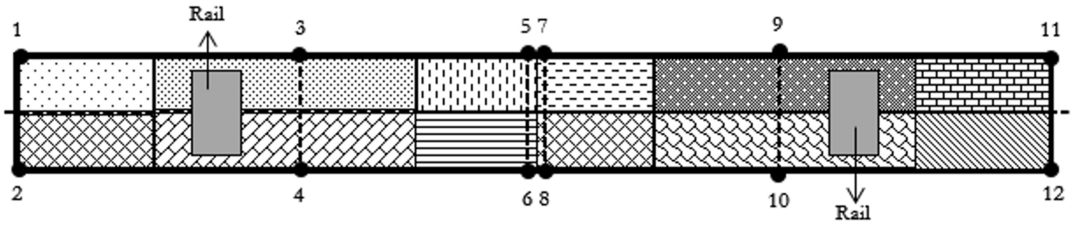

Fig. 9. LVDT locations on the sleeper to analyze permanent settlement by area-weighted method.

Table 5. Ballast proportions and their corresponding index properties tested in SRTF

Test label	Composition (%)		Density (kg/m^3)		Specific gravity, G_s	Uniformity coefficient, C_u
	Fresh ballast	Recycled ballast	Loose	Dense		
Fresh 1	100	0	1,345	1,573	2.67	1.152
Fresh 2	100	0	1,362	1,584	2.68	1.408
Reused 1	0	100	1,396	1,626	2.72	1.471
Reused 2	0	100	1,312	1,550	2.77	1.577
50:50 combination 1	50	50	1,384	1,575	2.70	1.547
50:50 combination 2	50	50	1,327	1,552	2.69	1.282

SRTF Results

The presentation and discussion of results uses the following definitions:

- permanent settlement is the irrecoverable vertical movement at the minimum load of 5 kN, which represents the minimum contact load at end of a load cycle; and
- spring stiffness is the change in vertical load per rail (sometimes termed per sleeper end) divided by the resilient deflection (units of kilonewtons per millimeter).

To obtain a single characteristic result for settlement and spring stiffness, the LVDT measurements were averaged for the whole sleeper using an area-weighted method (Fig. 8). Fig. 10 shows the

Table 6. Summary of SRTF tests

Test label (for graphs)	Sleeper type	Ballast grading	Ballast density (kg/m^3)	Shoulder slope	Total load cycles applied (million)
Baseline 1	Monoblock G44	NR 1	1,572.72	1:1	4.7
Baseline 2		NR 2	1,584.07		4.5
Reused 1		Recycled 1	1,586.17		4.5
Reused 2		Recycled 2	1,550.50		4.1
50:50 combination 1		Half NR + half recycled	1,574.69		4.2
50:50 combination 2			1,551.98		4.5

J. Geotech. Geoenviron. Eng., 2023, 149(1): 04022123

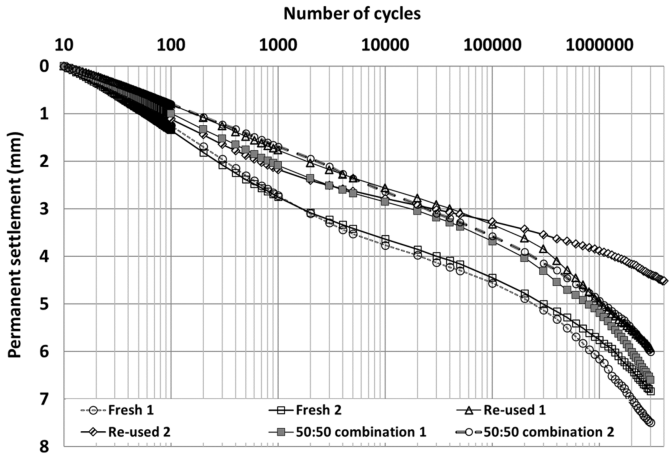

Fig. 10. Permanent settlement against number of loading cycles, zeroed after 10 cycles.

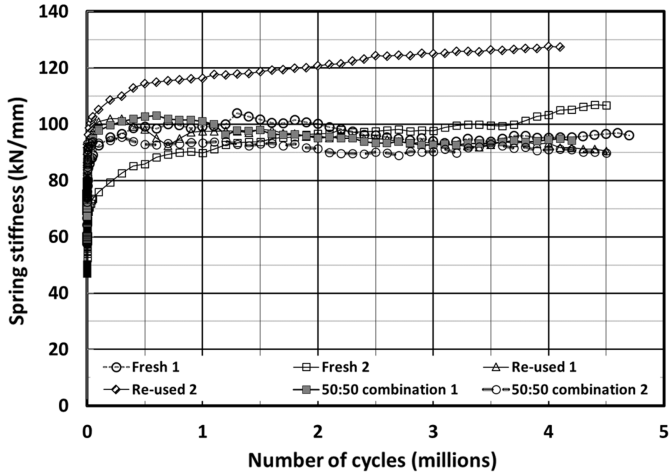

Fig. 11. Sleeper end spring stiffnesses based on area-weighted method.

average weighted permanent settlement versus the number of loading cycles on a logarithmic scale for all six tests. Zero on the y-axis corresponds to the sleeper level rezeroed after 10 loading cycles. The permanent settlement of fresh ballast was 20%–40% greater than that of the reused ballast after 3 million cycles of loading. The reused ballast consistently had smaller settlement with number of loading cycles than did the fresh ballast, whereas the 50:50 combination had settlement behavior somewhere between the two. Fig. 11 shows the spring stiffness with cycles. Each test showed an initial increase in average spring stiffness and subsequent stabilization with number of loading cycles. In previous work, lower spring stiffness has been shown to be associated with greater settlement (e.g., Abadi et al. 2018). However, in these tests the spring stiffness was very similar after it stabilized, with the exception of test Reused 2, which had consistently greater stiffness, and was the test with the lowest settlement. The permanent settlement continued until the end of the test, which was expected mainly due to the lateral spreading of the ballast (Abadi et al. 2015, 2018).

Triaxial Tests

Standard triaxial drained tests were carried out to compare the stress–strain behavior of fresh and life-expired ballast.

Test Arrangement

A large triaxial apparatus able to accommodate samples of 300 mm diameter and 450 mm height was used. This apparatus was similar to the one presented by Ng et al. (2002), which incorporated as a novel feature a differential pressure measurement system for volume change. Preparation of coarse-grained samples for triaxial testing requires particular modifications to usual triaxial testing procedures. The apparatus has to be large, and conventionally a maximum particle size–sample diameter ratio of no more than 6 is considered acceptable (Marachi et al. 1972) which was respected in these tests (Fig. 9). The large angular ballast grains require a thick membrane to prevent puncture during testing, and samples must be prepared so that they do not collapse or slump within the membrane prior to testing. Each sample was prepared using a controlled compactive effort to obtain repeatable initial density. To cope with these additional difficulties, a 4-mm-thick latex membrane was used and sealed against a steel cylindrical mold with an internal diameter of 308 mm. The ballast samples were placed into the mould in three layers, with each layer receiving 30 s of compactive effort from a vibrating disc placed onto the top surface. Two neoprene O-rings at the top platen and the cell base sealed the sample. Temporary suction of 20 kPa was applied while the mold was removed to retain the sample in its initial form (preventing collapse). The suction was retained until the sample had been placed into the apparatus and the cell was lowered over it. When the cell had been filled with water, the cell pressure was increased slowly as the suction progressively was released to avoid sample collapse and overstressing the sample compared with the intended effective confining stress for that test. Further details about the apparatus and a detailed sample preparation methodology were given by Aursudkij (2007).

Eight monotonic failure tests were carried out on different samples, and the results were processed to determine the mobilized angle of shearing resistance. A correction for membrane radial and axial stress was applied (Kuerbis and Vaid 1990). Each of the eight samples was prepared from sieved fractions to contain proportions of material at the median size fraction for each sieve interval (Fig. 9 and BSI 2002). This meant that unlike the rig tests, the density results can be compared directly, with any differences in initial density attributable mainly to the differing grain forms.

Triaxial Results

Figs. 12 and 13 plot the mobilized angle of shearing and the volumetric strain with axial strain for cell pressures of 30 and 60 kPa, respectively. The mobilized angle of shearing for reused ballast samples tended to have slightly higher values ($\sim +3°$) compared with those for the fresh samples at both stress magnitudes [Figs. 12(a) and 13(a)]. The volumetric strain of the reused material showed initial compression followed by dilation beyond 2% axial strain, whereas the fresh ballast had an initially flat volumetric response followed by steady dilation (from 1% axial strain) [Figs. 12(b) and 13(b)]. The fresh and used ballast exhibited similar rates of dilation ($d_{\varepsilon \mathrm{vol}}/d\gamma$), as indicated by the broadly parallel lines in Figs. 12(b) and 13(b) beyond 2% axial strain. The tests showed that the used ballast had a greater shear strength and took longer to begin to dilate, which support the results from the SRTF. The measured maximum mobilized shearing angles for the eight tests are listed in Table 7 along with the initial sample density and void ratio. The reused ballast tests always have higher maximum mobilized shearing angles and lower void ratios. Although the samples all were prepared using the same compactive effort, the reused samples always were fractionally denser. Ahmed and Martinez (2021) conducted triaxial tests to study the effect of particle shape on granular material, and observed that rounded sands begin to

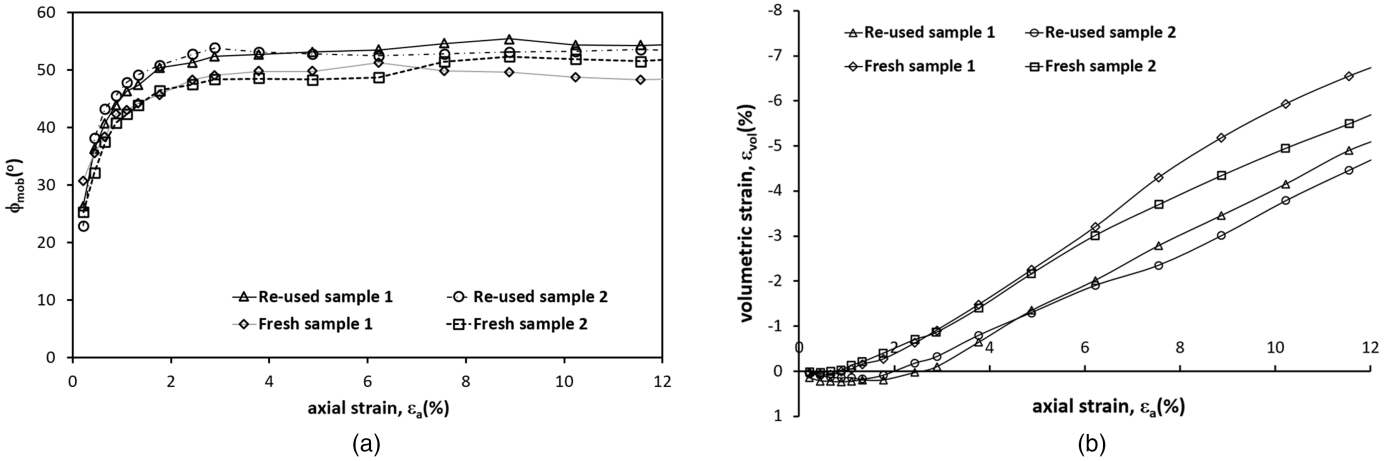

Fig. 12. Monotonic triaxial test results of fresh and used ballast tested at cell pressure of 30 kPa: (a) mobilized angle of shearing; and (b) volumetric strain response.

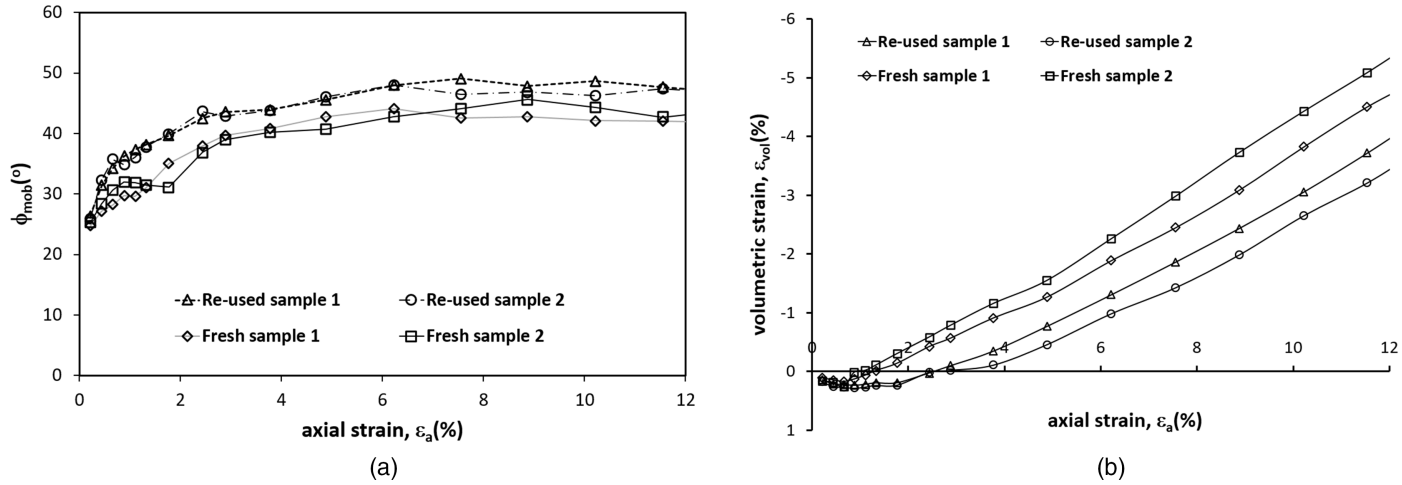

Fig. 13. Monotonic triaxial test results of fresh and used ballast tested at cell pressure of 60 kPa: (a) Mobilized angle of shearing; and (b) volumetric strain response.

Table 7. Summary of triaxial test specimen details and results

Cell pressure (kPa)	Ballast	Max mobilized angle of shearing (degrees)	Rate of dilation, $d_{\varepsilon vol}/d\gamma$	Initial weight (kg)	Initial density (kg/m^3)	Initial void ratio
30	Reused 1	55	0.52	51.78	1,628	0.62
	Reused 2	54	0.47	50.89	1,600	0.64
	Fresh 1	51	0.61	48.48	1,524	0.73
	Fresh 2	52	0.60	49.36	1,552	0.69
60	Reused 1	49	0.36	51.24	1,610	0.63
	Reused 2	48	0.33	50.67	1,592	0.70
	Fresh 1	44	0.49	49.31	1,550	0.70
	Fresh 2	46	0.53	48.26	1,517	0.73

dilate beyond 2% axial strain, whereas angular sands begin dilation at low strains without undergoing any compression stage.

The samples were sieved and weighed following the tests, which revealed the generation of new smaller fragments. The smallest grain size before the tests was 22.4 mm. Fig. 14 shows the mass passing sieve sizes less than 22.4 mm after the tests. The results show that although there was very little breakage (less than 0.5 kg of material in all cases), the breakage of fresh ballast was proportionally greater than that of the reused ballast at both stress levels. Breakage is likely to be a function of the fracture strength of the grains and the work done (indicated by volume change or dilation) on the ballast during testing. More dilation occurred in the fresh tests, which may tend to abrade or break grains.

Discussion

The reused ballast in this study contained 63% granite and 21% basalt (Table 1). Studies of strength of intact basalt and granite rocks by Hoek and Brown (1992) and Piasta et al. (2017) showed that the compressive strength and modulus of elasticity of basalt rocks is greater than that of granite. This is mainly because granite is made up of less quartz (~35% quartz, 40% feldspar), whereas basalt is 90% quartz (Fig. 2 and Table 3). The overall strength and mobilized shearing resistance of the reused ballast might have been

J. Geotech. Geoenviron. Eng., 2023, 149(1): 04022123

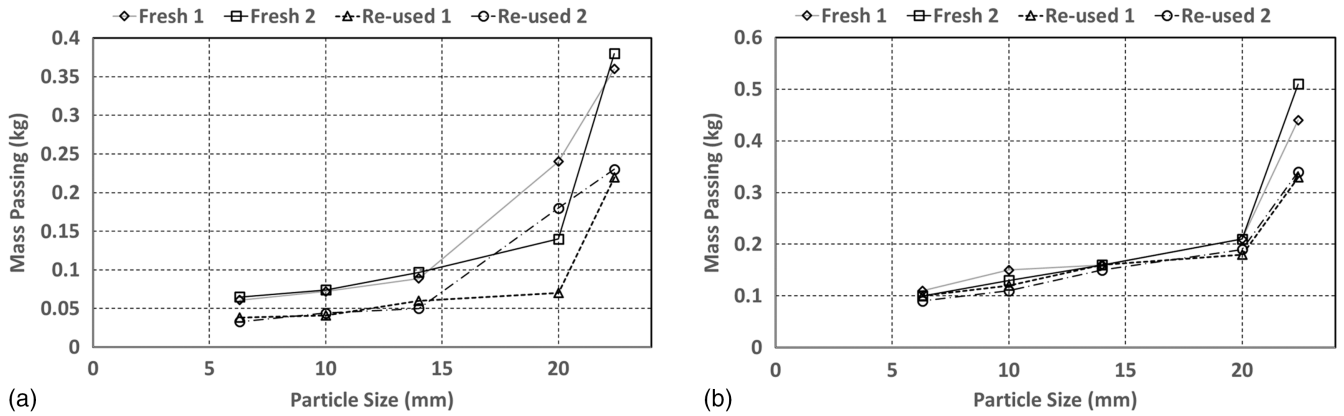

Fig. 14. Mass of broken asperities smaller than 22.4 mm: (a) 30 kPa; and (b) 60 kPa.

improved by the presence of the basalt grains, compared with fresh ballasts formed solely of granite and granodiorite. Compared with other triaxial tests in the literature, these shear strengths fall within the range of expected behavior (e.g., Aursudkij et al. 2009; Indraratna et al. 1998; Suiker et al. 2005; Raymond and Davies 1978). The only other triaxial tests of used ballasts that the authors found were carried out by Ionescu and Indraratna (2003), who compared recovered ballast and a fresh ballast formed of a volcanic basalt (latite). The recovered material was reported as having a 61% angular crushed rock composition and a further 35% crushed river gravel. In their tests the fresh ballast outperformed the recovered material, which was attributed mainly to greater volumetric deformation of the recovered material. This result, which was the opposite of that found in the present tests, highlights that not all recovered material is the same. There also is likely to be a significant relative difference in different fresh ballasts, so that even if a reused ballast appears to perform comparatively well compared with one type of fresh ballast, other fresh ballasts could perform better. In our 50:50 ballast tests we mixed the fresh and life-expired ballast in small batches of 100 kg each to obtain an even mix with hand shovel. Because ballast normally is transported using 1-t bags, we would recommend pouring out both the fresh and spent ballast materials simultaneously from the 1-t bags and mixing the pile manually or using a mixing machine or excavator.

The greater sphericity and the reduced angularity and surface roughness of reused ballast affects its initial packing density and shear behavior. These tests showed that, collectively, the competing influence of these grain characteristics leads to greater initial density, (lower void ratio) suppressing initial dilation and generating a stable support stiffness in the SRTF. Fresh ballast, with its lower sphericity and greater angularity and surface roughness, had a lower initial packing density (higher void ratio) and earlier onset of a dilative response when sheared. The greater volumetric change of the fresh ballast was evident from the particle breakage analysis carried out after each test, in which fresh ballast had greater breakage than reused ballast. Thus, the life-expired ballast can be reused alone or mixed with fresh ballast as long as it is cleaned (without any fouling material) and graded to the trackbed design standards.

Conclusions

The petrographic analysis showed that the majority of the recovered material was granite (60%) with 21% basalt, and therefore it was acceptable to compare its performance with that of a fresh ballast mainly formed of granite. The form analysis showed that there was a small tendency for more-spherical columnar grains in the reused material. The surface roughness analysis showed that there was a major reduction of the roughness of the used ballast compared with the fresh ballast.

In the SRTF tests the reused ballast performed best in terms of having the least permanent settlement compared with the fresh and blended ballasts. Counterintuitively, the fresh material settled the most.

The monotonic triaxial tests results showed that the reused ballast exhibited slightly higher shear strength, had greater initial densities compared with the fresh ballast, and dilated less. The monotonic failure results support the SRTF results.

Taken as a whole, the three strands of this research indicate that a reused ballast appears to perform slightly better than a particular fresh ballast of similar mineral composition. The reduced surface roughness of the used ballast was more than compensated for by other improvements—e.g., the greater initial packing density. The presence of basalt contributed to the increase in strength and mobilized angle of shearing resistance of the reused ballast.

In general, there is no reason not to reuse ballast if it can be cleaned and screened and supplied in an acceptable particle-size distribution, and its mineral composition confirms that it is suitable. The performance of the reused ballast then should be similar to that of fresh ballast of similar mineral composition. The reuse of material potentially is more sustainable and less costly—although this may depend on local circumstances. Ideally, further work should compare the in-field performance of reused and fresh ballast at control sites.

Data Availability Statement

All data, models, and code generated or used during the study appear in the published article.

Acknowledgments

The work described in this paper was jointly funded by the EU via the project In2Rail (Call identifier H2020-MG-2014, Grant Agreement No. 635900) and the UK's Engineering and Physical Sciences Research Council (EPSRC) as part of the track to the future (T2F) project (Grant Reference EP/M025276/1). The authors thank Network Rail for support in kind (providing the materials for testing and explaining current practice). The authors also acknowledge staff at the UK's National Oceanography Centre (NOC) for the mineralogical analyses, in particular Dr. Richard Pearce and Dan Doran.

References

Abadi, T., L. Le Pen, A. Zervos, and W. Powrie. 2015. "Measuring the area and number of ballast particle contacts at sleeper/ballast and ballast/subgrade interfaces." *Int. J. Railway Technol.* 4 (Jan): 45–72. https://doi.org/10.4203/ijrt.4.2.

Abadi, T., L. Le Pen, A. Zervos, and W. Powrie. 2018. "Improving the performance of railway tracks through ballast interventions." *Proc. Inst. Mech. Eng., Part F: J. Rail Rapid Transit* 232 (5): 337–355. https://doi.org/10.1177/0954409716671545.

Abadi, T., L. Le Pen, A. Zervos, and W. Powrie. 2019. "Effect of sleeper interventions on railway track performance." *J. Geotech. Geoenviron. Eng.* 145 (4): 04019009. https://doi.org/10.1061/(ASCE)GT.1943-5606.0002022.

Ahmed, S. S., and A. Martinez. 2021. "Triaxial compression behavior of 3D printed and natural sands." *Granular Matter* 23 (4): 82. https://doi.org/10.1007/s10035-021-01143-0.

Aingaran, S., L. Le Pen, A. Zervos, and W. Powrie. 2018. "Modelling the effects of trafficking and tamping on scaled railway ballast in triaxial tests." *Transp. Geotech.* 15 (4): 84–90. https://doi.org/10.1016/j.trgeo.2018.04.004.

Aursudkij, B. 2007. "A laboratory study of railway ballast behaviour under traffic loading and tamping maintenance." Doctor of Philosophy, Dept. of Civil Engineering, Univ. of Nottingham.

Aursudkij, B., G. R. McDowell, and A. C. Collop. 2009. "Cyclic loading of railway ballast under triaxial conditions and in a railway test facility." *Granular Matter* 11 (Jan): 391–401. https://doi.org/10.1007/s10035-009-0144-4.

Barrett, P. J. 1980. "The shape of rock particles, a critical review." *Sedimentology* 27 (8): 291–303. https://doi.org/10.1111/j.1365-3091.1980.tb01179.x.

BSI (British Standards Institution). 2002. *Aggregate for railway ballast*. BS EN 13450. London: BSI.

BSI (British Standards Institution). 2011. *Tests for mechanical and physical properties of aggregates, Part 1: Determination of the resistance to wear (micro Deval)*. BS EN 1097-1. London: BSI.

BSI (British Standards Institution). 2020. *Tests for mechanical and physical properties of aggregates, Part 2: Method for the determination of resistance to fragmentation*. BS EN 1097-2. London: BSI.

Cho, G.-C., J. Dodds, and J. C. Santamarina. 2006. "Particle shape effects on packing density, stiffness and strength: Natural and crushed sands." *J. Geotech. Geoenviron. Eng.* 132 (5): 591–602. https://doi.org/10.1061/(ASCE)1090-0241(2006)132:5(591).

Clayton, C. R. I., M. C. Matthews, and N. E. Simons. 1995. *Site investigation: A handbook for engineers*. Hoboken, NJ: Blackwell Science.

Clifton, A. W., M. J. Klassen, and B. R. Watters. 1987. "Production and testing of ballast." In *Performance of aggregates in railroads and other track performance*, 26–34. Washington, DC: Transportation Research Board.

Gong, Y., S. T. Misture, P. Gao, and N. P. Mellott. 2016. "Surface roughness measurements using power spectrum density analysis with enhanced spatial correlation length." *J. Phys. Chem. C* 120 (5): 22358–22364. https://doi.org/10.1021/acs.jpcc.6b06635.

Harkness, J., and A. Zervos. 2019. "Some effects of particle shape on the mechanical behaviour of granular materials." In *DEM8: 8th Int. Conf. on Discrete Element Methods*. Enschede, Netherlands: Univ. of Twente.

Harkness, J., A. Zervos, L. Le Pen, S. Aingaran, and W. Powrie. 2016. "Discrete element simulation of railway ballast: Modelling cell pressure effects in triaxial tests." *Granular Matter* 18 (8): 65. https://doi.org/10.1007/s10035-016-0660-y.

Hoek, E., and E. T. Brown. 1997. "Practical estimates of rock mass strengths." *Int. J. Rock Mech. Min. Sci.* 34 (8): 1165–1186. https://doi.org/10.1016/S1365-1609(97)80069-X.

Indraratna, B., D. Ionescu, and H. D. Christie. 1998. "Shear behavior of railway ballast based on large-scale triaxial tests." *J. Geotech. Geoenviron. Eng.* 124 (5): 439. https://doi.org/10.1061/(ASCE)1090-0241(1998)124:5(439).

Indraratna, B., and W. Salim. 2003. "Deformation and degradation mechanics of recycled ballast stabilised with geosynthetics." *Soils Found.* 43 (85): 35. https://doi.org/10.3208/sandf.43.4_35.

Ionescu, D., and B. Indraratna. 2003. "Behaviour of recycled railway ballast based on large-scale triaxial tests." In *Proc., 6th Railway Engineering*, 124–136. Edinburgh, Scotland: Engineering Technics Press.

Kuerbis, R. H., and Y. P. Vaid. 1990. "Corrections for membrane strength in the triaxial test." *Geotech. Test. J.* 13 (Jan): 361–369. https://doi.org/10.1520/GTJ10179J.

Le Pen, L., and W. Powrie. 2011. "Contribution of base, crib, and shoulder ballast to the lateral sliding resistance of railway track: A geotechnical perspective." *J. Rail Rapid Transit* 225 (5): 113–129. https://doi.org/10.1177/0954409710397094.

Le Pen, L., W. Powrie, A. Zervos, S. Ahmed, and S. Aingaran. 2013. "Dependence of shape on particle size for a crushed rock railway ballast." *Granular Matter* 15 (6): 849–861. https://doi.org/10.1007/s10035-013-0437-5.

Le Pen, L., G. Watson, A. Hudson, and W. Powrie. 2018. "The behaviour of under-sleeper pads at switches and crossings—Field measurements." *Proc. Inst. Mech. Eng., Part F: J. Rail Rapid Transit* 232 (4): 1049–1063. https://doi.org/10.1177/0954409717707400.

Li, D., and E. T. Selig. 1998a. "Method for railroad track foundation design. I: Development." *J. Geotech. Geoenviron. Eng.* 124 (4): 316–322. https://doi.org/10.1061/(ASCE)1090-0241(1998)124:4(316).

Li, D., and E. T. Selig. 1998b. "Method for railroad track foundation design. II: Applications." *J. Geotech. Geoenviron. Eng.* 124 (4): 323–329. https://doi.org/10.1061/(ASCE)1090-0241(1998)124:4(323).

Madhusudhan, B. N., and M. C. Todisco. 2018. "Does G0 of granular materials carry information on their particle characteristics?" In *Micro to MACRO mathematical modelling in soil mechanics*, 235–245. Berlin: Springer.

Marachi, N. D., C. K. Chan, and H. B. Seed. 1972. "Evaluation of properties of rockfill materials." *J. Soil Mech. Found. Div.* 98 (1): 95–114. https://doi.org/10.1061/JSFEAQ.0001735.

Ng, C. W. W., L. T. Zhan, and Y. J. Cui. 2002. "A new simple system for measuring volume changes in unsaturated soils." *Can. Geotech. J.* 39 (5): 757–764. https://doi.org/10.1139/t02-015.

Piasta, W., J. Góra, and W. Budzyński. 2017. "Stress-strain relationships and modulus of elasticity of rocks and of ordinary and high performance concretes." *Constr. Build. Mater.* 153 (7): 728–739. https://doi.org/10.1016/j.conbuildmat.2017.07.167.

Potticary, M. 2018. "A numerical investigation of the effect of particle shape on the strength of coarse granular materials." Ph.D. thesis, Dept. of Civil, Maritime and Environment Engineering Sciences, Univ. of Southampton.

Potticary, M., A. Zervos, and J. Harkness. 2014. "A numerical investigation into the effect of particle form on the strength of granular materials." In *Proc., 22nd UK National Conf. of the Association for Computational Mechanics in Engineering*. Exeter, UK: Infrastructure Group.

Potticary, M., A. Zervos, and J. Harkness. 2015. "An investigation into the effect of particle platyness on the strength of granular materials using the discrete element method." In *Proc., Int. Conf. on Particle-based Methods*. Barcelona, Spain: International Center for Numerical Methods in Engineering.

Potticary, M., A. Zervos, and J. Harkness. 2016. "The effect of particle elongation on the strength of granular materials." In *Proc., 24th Conf. on Computational Mechanics*. Cardiff, Wales: Cardiff Univ.

Qian, Y., E. Tutumluer, Y. M. A. Hashash, and J. Ghaboussi. 2022. "Triaxial testing of new and degraded ballast under dry and wet conditions." *Transp. Geotech.* 34 (May): 100744. https://doi.org/10.1016/j.trgeo.2022.10074.

Raymond, G. P. 1985. "Research on rail road ballast specification and evaluation." *Transp. Res. Rec.* 1006 (1): 1–8.

Raymond, G. P., and J. R. Davies. 1978. "Triaxial tests on dolomite railroad ballast." *J. Geotech. Eng. Div.* 104 (8): 737–751. https://doi.org/10.1061/AJGEB6.0000646.

Selig, E. T., and D. L. Boucher. 1990. "Abrasion tests for railroad ballast." *Geotech. Test. J.* 13 (8): 301. https://doi.org/10.1520/GTJ10173J.

Selig, E. T., and J. M. Waters. 1994. *Track geotechnology and substructure management*. London: Telford.

Suiker, A. S. J., E. T. Selig, and R. Frenkel. 2005. "Static and cyclic triaxial testing of ballast and subballast." *J. Geotech. Geoenviron. Eng.* 131 (6): 771–782. https://doi.org/10.1061/(ASCE)1090-0241(2005)131:6(771).

Watters, B., M. Klassen, and A. Clifton. 1987. "Evaluation of ballast materials using petrographic criteria." *Transp. Res. Rec.* 1131 (Jan): 45–63.

Zingg, T. 1935. "Beitrage Zur Schotteranalyse." *Schweiz Miner. Petrog. Mitt* 15 (Apr): 37–140. https://doi.org/10.3929/ethz-a-000103455.